Available online at www.sciencedirect.com
ScienceDirect
Nuclear Physics B Proceedings Supplement 00 (2014) 1–6
Nuclear Physics B Proceedings Supplement

Soft QCD and underlying event measurements at ATLAS

Oleg Zenin[a,1], on behalf of the ATLAS Collaboration

[a] *IHEP, Protvino, Russian Federation*

Abstract

Recent soft QCD results obtained in pp collisions at $\sqrt{s} = 7$ TeV with ATLAS detector at the LHC are presented. These include measurement of inclusive $\phi(1020)$-meson production cross section, measurements of underlying event in inclusive jet and Z-boson events, and a direct study of double-parton scattering using $W+2$jet events. The discussed measurements can be used to develop and tune models of soft hadroproduction.

Keywords: Soft QCD, non-perturbative, underlying event, multiple parton interactions, pp scattering, 7 TeV, ATLAS, LHC

1. The differential production cross section of the $\phi(1020)$-meson

Measurements of the $\phi(1020)$-meson probe strangeness production at a soft scale $Q \sim 1$ GeV and constrain s-quark and gluon densities at low-x, as well as fragmentation models. Presented is the measurement [1] with the ATLAS detector [2] of the $\phi(1020)$-meson production cross section in pp interactions at $\sqrt{s} = 7$ TeV, using the $\phi \to K^+K^-$ decay mode. Both kaons were identified by their energy loss in the ATLAS tracking system to reduce combinatorial backgrounds (Fig. 1). The cross section is measured in bins of $\phi(1020)$-meson transverse momentum, $p_{T,\phi}$ (Fig. 2a) and rapidity, y_ϕ (Fig. 2b). To avoid model-dependent extrapolations outside the detector acceptance, the fiducial volume of the measurement is defined as $500 < p_{T,\phi} < 1200$ MeV, $|y_\phi| < 0.8$, $p_{T,K^\pm} > 230$ MeV and $p_{K^\pm} < 800$ MeV. The data sample was taken in April 2010 at $\sqrt{s} = 7$ TeV, with an integrated luminosity of 383 μb^{-1}.

The signal was extracted by a χ^2 fit to the K^+K^- invariant mass spectrum, $m_{K^+K^-}$, performed in each region of the phase space after applying corrections for track selection efficiency. The signal shape is parameterised by relativistic Breit-Wigner function convolved with the Gaussian resolution function. The background is described by an empirical smooth function of $m_{K^+K^-}$ constrained by fitting the sample with two kaons of the same charge.

The cross section σ^i_{bin} in i-th bin of the phase space is determined as $\sigma^i_{bin} = N_i/\mathcal{L}$, where $\mathcal{L}$ is the integrated luminosity and N_i is the number of efficiency-corrected reconstructed $\phi \to K^+K^-$ candidates in i-th bin.

The fiducial cross section was compared to a number of MC models. The best description is achieved with `Pythia 6 DW` tune, as well as with `EPOS-LHC` tune (Fig. 2). Other models demonstrate a large spread of predictions, thus indirectly confirming the constraining power of the measurement.

In order to allow comparison with other measurements, the fiducial cross section was extrapolated to a cross section in the kinematic region $500 < p_{T,\phi} < 1200$ MeV and $|y_\phi| < 0.5$, using Pythia 6 MC particle level data. The MC model dependent variation of the acceptance correction factor is estimated to be 10% and assigned to the systematic uncertainty of the extrapolated cross section. The result is compared to the measurement [3] by the ALICE Collaboration (Fig. 3). Both results are in an agreement within the systematic uncer-

[1] ozenin@cern.ch

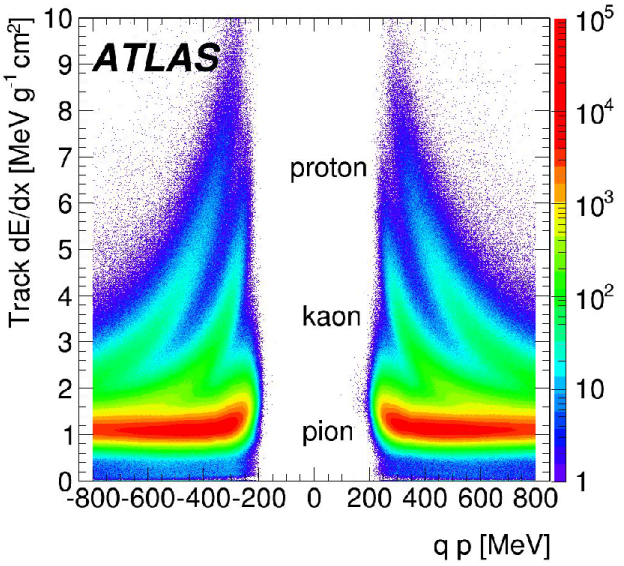

Figure 1: The truncated mean (see [1] for details) for the energy loss per track as a function of signed momentum of selected tracks.

tainties.

2. Underlying event in jet events

Hard pp collisions at LHC energies typically involve, besides a primary parton-parton interaction at a high energy scale, several softer interactions including additional parton-parton scatters termed multiple parton interactions (MPI), fragmentation of QCD strings connecting outgoing coloured objects including beam remnants, initial and final state radiation. This activity not directly associated with the primary parton-parton scattering is commonly termed "underlying event" (UE). In a naïve event picture (Fig. 4), regions well separated in a phase space from the hard final state objects are believed to be most sensitive to the UE.

The measurement of UE observables in inclusive jet and exclusive di-jet events [4] was performed in ATLAS experiment using pp collisions at $\sqrt{s} = 7$ TeV. The data sample corresponding to 37 pb^{-1} of integrated luminosity was collected in 2010. The orientation of the hard scatter is defined by the hardest jet whose transverse momentum, p_T^{lead} sets the scale of the hard process. Jets are reconstructed using the ATLAS calorimeter and required to have $p_T > 20$ GeV and $|y| < 2.8$. The leading-jet transverse momentum covers the range $p_T^{lead} = 20$–800 GeV. The UE is characterised by charged particle multiplicity, charged and inclusive Σp_T per $\eta - \phi$ unit area, and mean p_T of a charged particle. These observables are constructed using prompt stable charged

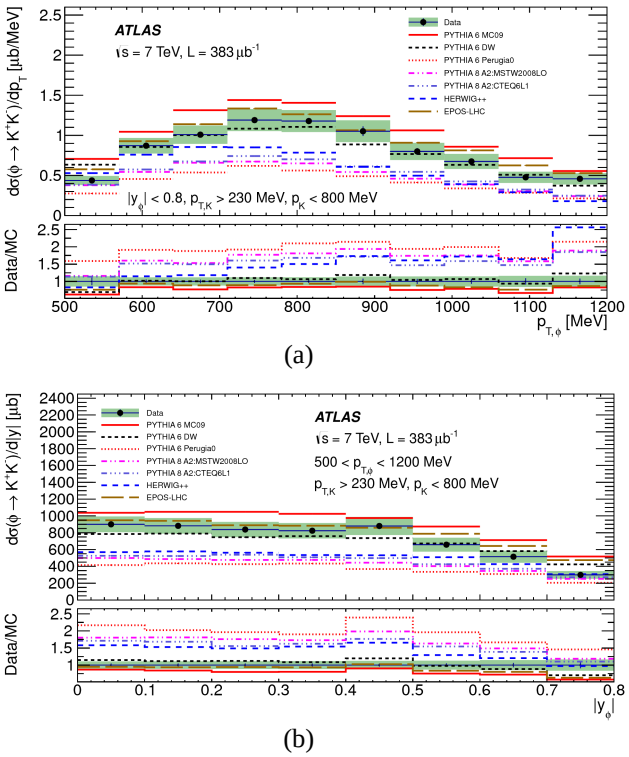

Figure 2: The $\phi(1020) \to K^+K^-$ cross section in the fiducial region [1] as a function of $p_{T,\phi}$ (a) and $|y_\phi|$ (b). The error bars represent the statistical uncertainty and the green band represents the quadratic sum of the statistical and systematic uncertainties. The 3.5% luminosity uncertainty is not included. The data are compared to various MC models as described in the legends.

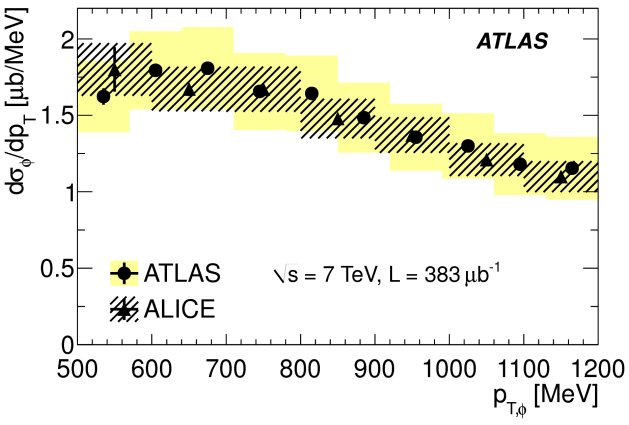

Figure 3: The $\phi(1020)$-meson cross section as a function of $p_{T,\phi}$, extrapolated using `Pythia 6` to the kinematic region with $500 < p_{T,\phi} < 1200$ MeV and $|y_\phi| < 0.5$ [1], is compared to the ALICE result [3]. The error bars represent the statistical uncertainty and the bands represent the quadratic sum of statistical and systematic uncertainties. The 3.5% luminosity uncertainty is not included.

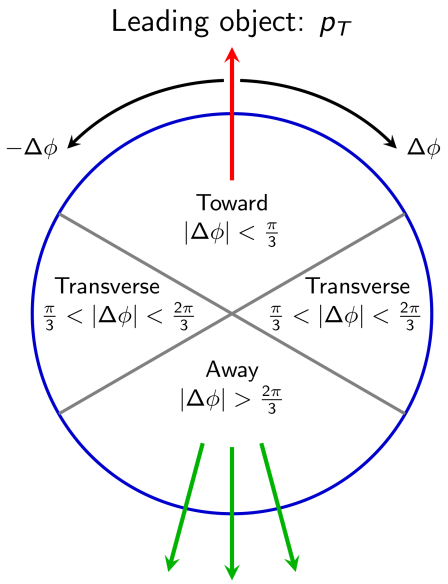

Figure 4: Definition of the UE regions as a function of the azimuthal angle with respect to the leading object [4, 5].

particles populating the transverse region covering the azimuthal range $\pi/3 \leq |\Delta\phi| \leq 2\pi/3$ from the leading jet (Fig. 4). To further discriminate between the UE and additional jet activity, the full transverse region is divided into two one-side sectors, "trans-max" and "trans-min" selected in each event according to which one has more or less activity. The latter is characterised by the multiplicity or Σp_T for the respective observables. Charged particles reconstructed in ATLAS tracking system are selected with $p_T > 500$ MeV and $|\eta| < 2.5$. Inclusive transverse energy flow of charged particles with $p > 500$ MeV and neutral particles with $p > 200$ MeV is measured using calorimeter clusters in the pseudorapidity range extended to $|\eta| < 4.8$.

The evolution of the charged Σp_T density with the hard scale p_T^{lead} in inclusive jet events is shown on Fig. 5a. Additional jets produced in the hard process contaminate "trans-max" region more than "trans-min", as indicated by the increase of "trans-max" Σp_T with p_T^{lead} and an approximate constancy of "trans-min" Σp_T, respectively. In exclusive di-jet events both "trans-max" and "trans-min" Σp_T develop a p_T^{lead}-independent plateau (Fig. 5b). A slight decrease of "trans-min" activity with p_T^{lead} is more pronounced in the extended pseudorapidity range (Fig. 6) where none of the MC models reproduces the trend well. The behaviour of UE activity in exclusive di-jet events shows that pure MPI activity can be modelled to some extent as independent

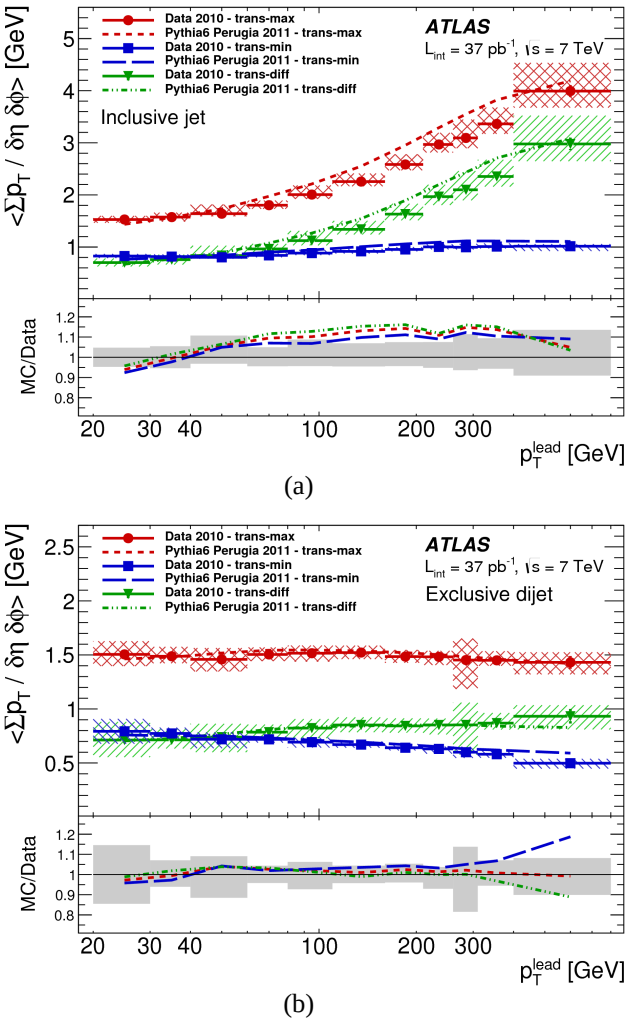

Figure 5: Charged Σp_T density in trans-max and trans-min regions as a function of the leading-jet p_T in inclusive jet (a) and exclusive di-jet (b) events [4].

of the hard process scale, given that the latter is high enough to ensure that pp collisions were central.

Although MC models provide satisfactory predictions of UE observables in the central $|\eta| < 2.5$ range, the discrepancies seen in the extended range $|\eta| < 4.8$ open the possibility to further improve the UE models.

3. Underlying event in inclusive Z-boson events

Another UE measurement complementary to the one discussed in the previous section was performed with ATLAS detector using inclusive Z-boson events at $\sqrt{s} =$ 7 TeV [5]. The full 2011 dataset was used, corresponding to 4.6 pb^{-1} integrated luminosity. Z-bosons

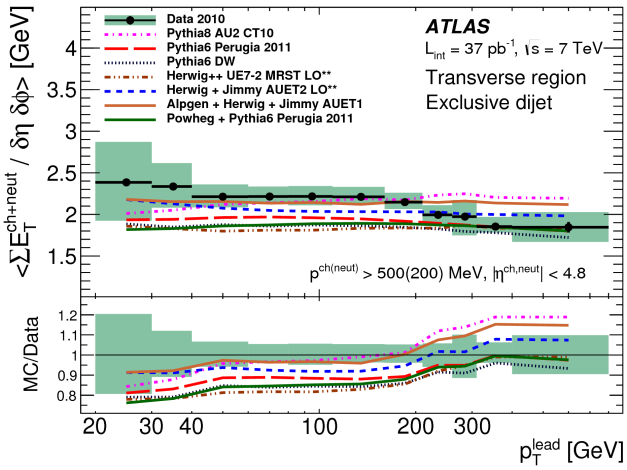

Figure 6: Charged and neutral ΣE_T density in the full transverse region measured in exclusive di-jet events in the full calorimeter acceptance $|\eta| < 4.8$ [4].

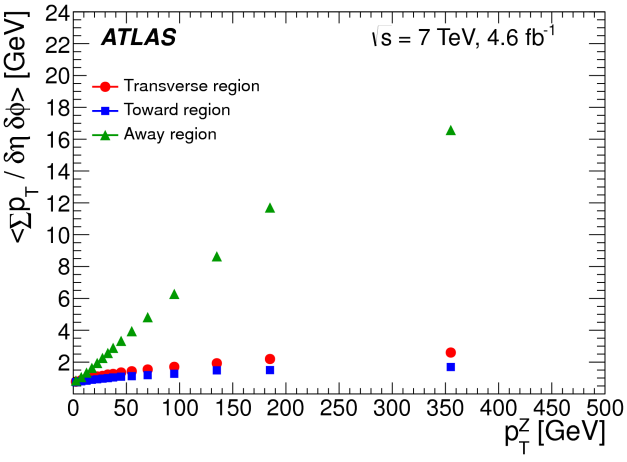

Figure 7: Charged Σp_T density as a function of Z-boson transverse momentum, p_T^Z, in the full transverse, toward and away regions [5].

were reconstructed in e^+e^- and $\mu^+\mu^-$ decay modes, with the transverse momentum, p_T^Z, ranging from zero to 0.5 TeV. The UE observables, charged particle multiplicity and Σp_T per unit $\eta-\phi$ area, as well as mean p_T of a charged particle were measured in previously defined azimuthal regions (Fig. 4) as functions of the hard scale p_T^Z. The observables were constructed using prompt stable charged particles with $p_T > 500$ MeV and $|\eta| < 2.5$ (excluding the di-lepton pair from Z-boson decay) reconstructed in the ATLAS tracking system.

In contrast to the UE analysis in jet events, in this analysis the azimuthal region towards the leading object is also sensitive to the UE, due to absence of QCD FSR from the leptonically decaying Z-boson (Fig. 7).

The results in the transverse region are similar to the ones obtained in inclusive jet events (Fig. 8). An apparent difference in the "trans-max" region is attributed to selection bias in the Z UE analysis, where no cut on p_T of additional jets was applied, contrary to the jet UE analysis where p_T of additional jets could not exceed p_T of the leading jet. A remarkable conincidence of charged particle multplicity and Σp_T densities in the "trans-min" region suggests that UE properties depend rather on the scale of the hard process than on the colour configuration of the final state.

A universal nature of the UE is also indicated by similarity of the soft part of differential "trans-min" Σp_T distributions (unaffected by previously mentioned kinematic selection bias) in jet and Z-boson events (Fig. 9).

The original paper [5] contains numerous plots comparing the measured UE distributions with the predictions of several MC models. The models provide a qualitatively good description of the data, but with some significant discrepancies giving precise information sensitive to the choice of parameters used in the various UE models.

4. Double-parton scattering in W + 2jet events

At LHC energies, the rate of multiple parton interactions (MPI) becomes non-negligible due to an increase of PDFs at lower x values. This gives rise to sizeable backgrounds to many physically interesting final states produced in a single-parton scattering. The presented ATLAS analysis [6] extracts the fraction of W + 2jets events where W-boson and the two jets were produced in double-parton interactions (DPI). The analysis utilises a sample of $W \to e\nu$ and $W \to \mu\nu$ events collected in pp collisions in 2010, with an integrated luminosity of 36 pb^{-1}. Calorimeter jets were required to have $p_T > 20$ GeV and $|y| < 2.8$. To determine the double-parton contribution to the W + 2jet sample, the analysis employs a template fit of the variable $\Delta^n_{jets} = |\vec{p}_{T,jet1} + \vec{p}_{T,jet2}|/(|\vec{p}_{T,jet1}| + |\vec{p}_{T,jet2}|)$ quantifying the balance of the transverse momentum in the di-jet system. The Δ^n_{jets} templates were constructed using W+jets MC samples generated with Alpgen+Herwig+Jimmy MC with the DPI contribution switched on and off (Fig. 10).

A fit to the data (Fig. 11) yields the DPI fraction $f_{DPI} = 0.08 \pm 0.01_{stat} \pm 0.02_{syst}$. The extracted fraction f_{DPI} was used to derive the effective area parameter, σ_{eff}, for hard double-parton scattering. As shown on Fig. 12, $\sigma_{eff} = 15 \pm 3_{stat.}{}^{+5}_{-3}{}_{syst.}$ is consistent with the measurements at lower energies.

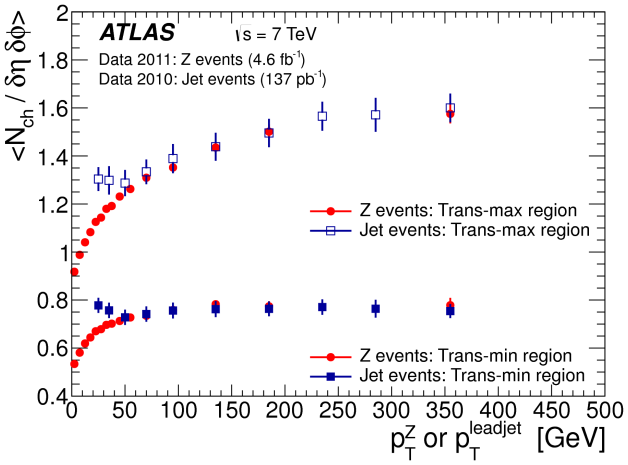

(a)

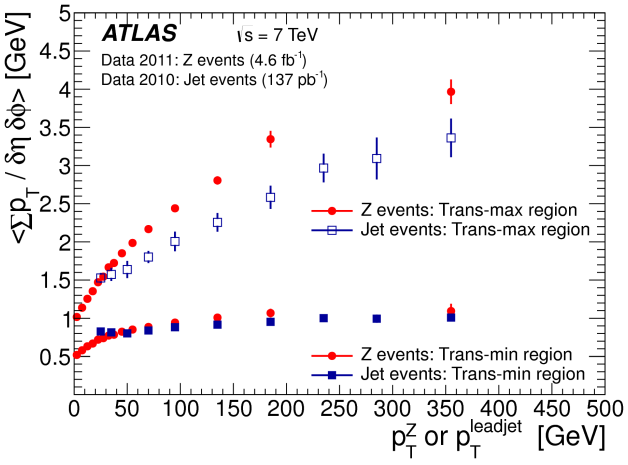

(b)

Figure 8: Charged particle multiplicity (a) and Σp_T (b) densities compared between inclusive jet and Z-boson events, respectively as functions of the leading jet transverse momentum, $p_T^{lead\,jet}$ and Z-boson transverse momentum, p_T^Z , in the transverse, "trans-max" and "trans-min" regions [5].

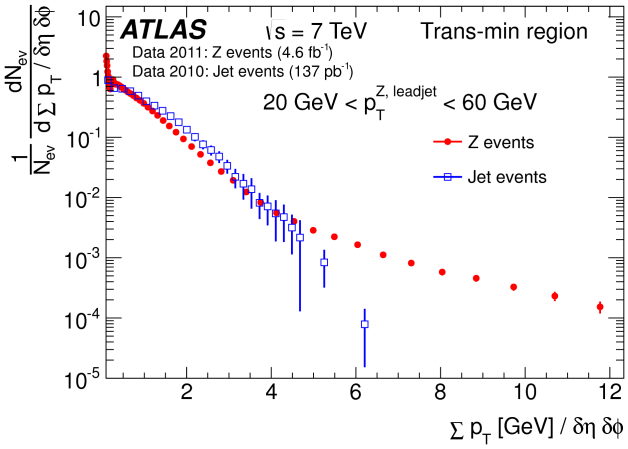

Figure 9: Distributions of charged particle Σp_T density, compared between jet and Z-boson events, respectively in Z-boson transverse momentum, p_T^Z and leading jet transverse momentum, $p_T^{lead\,jet}$ interval between 20-60 GeV, in the "trans-min" region [5].

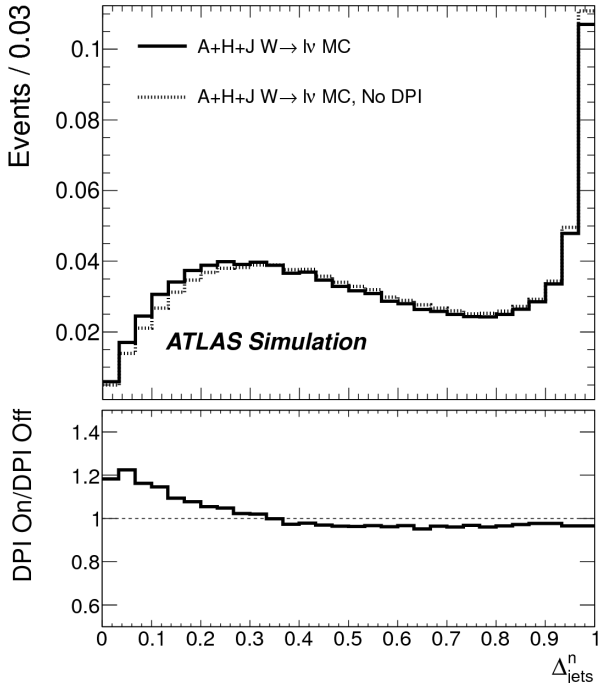

Figure 10: Comparison of Δ^n_{jets} shapes, at detector level, for selected $W(\ell\nu)$+2jet events as predicted by Alpgen+Herwig+Jimmy MC, with DPI on and off [6].

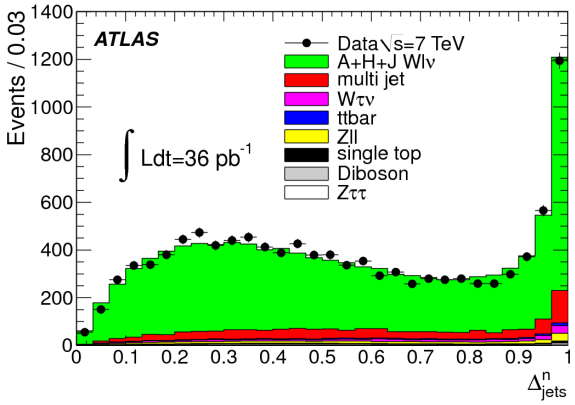

Figure 11: The Δ^n_{jets} distribution at detector level for events passing the $W(\ell\nu)$ + 2jet selection cuts. The distribution from data (dots) is compared with Alpgen+Herwig+Jimmy signal MC (histogram) predictions. In addition, physics backgrounds, also shown, have been added in due proportion to the MC histogram [6].

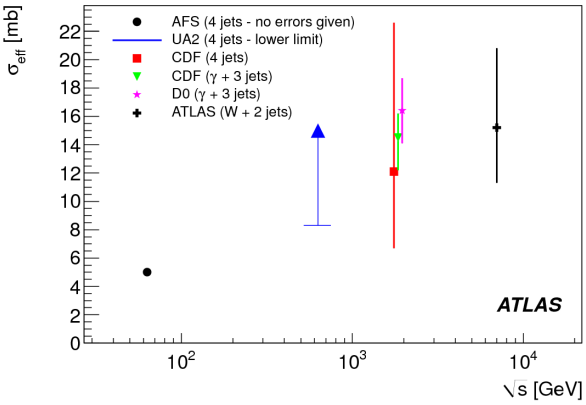

Figure 12: $\sqrt{s}$ dependence of σ_{eff} extracted in different processes in different experiments [6]. The error bars represent qudratically added statistical and systematic uncertainties.

References

[1] ATLAS Collaboration, Eur. Phys. J. C 74 (2014) 2895 [arXiv:1402.6162[hep-ex]]
[2] ATLAS Collaboration, JINST 3 (2008) S08003 [arXiv:0901.0512[hep-ex]]
[3] ALICE Collaboration, Eur. Phys. J. C 72 (2012) 2183 [arXiv:1208.5716[hep-ex]]
[4] ATLAS Collaboration, Eur. Phys. J. C 74 (2014) 2965 [arXiv:1406.0392[hep-ex]]
[5] ATLAS Collaboration, [arXiv:1409.3433[hep-ex]], sumbitted to Eur. Phys. J. C.
[6] ATLAS Collaboration, New J. Phys. 15 (2013) 033038 [arXiv:1301.6872[hep-ex]]